Original Article
Pancreatic neuroendocrine neoplasms: computed tomography features and the correlation to pathological tumor grade

Feng Jin[1,3], Kai Wang[2], Tingting Qin[4], Xin Li[3], Feng Guo[3], Qiqi Jiang[3], Yan Zou[3], Ping Han[3]

Departments of [1]Radiology, [2]Neurosurgery, The Affiliated Hospital of Inner Mongolia Medical University, Hohhot 010050, China; [3]Department of Radiology, Union Hospital, Tongji Medical College, Huazhong University of Science and Technology, 1277 Jiefang Avenue, Wuhan 430022, China; [4]Department of Epidemiology and Health Statistics, School of Public Health Tongji Medical College, Huazhong University of Science and Technology, 13 Hangkong Road, Wuhan 430030, China

Abstract: Objectives: To analyze the computed tomography (CT) features of pancreatic neuroendocrine neoplasms (pNENs) and to identify useful CT findings for differentiating tumors with different pathological grades. Materials and methods: Fifty patients with pNENs confirmed by postoperative pathology in our hospital from September 2012 to July 2016 who underwent preoperative plain and contrast-enhanced CT scans were included. CT features including tumor location, tumor size, shape, margins, growth pattern, pattern, CT attenuation values, enhancement patterns, degenerative changes, duct dilatation, peripancreatic tissue or vascular invasion, lymphadenopathy and metastases were evaluated. One-way ANOVA, the Kruskal-Wallis test, Fisher's exact test and ROC analysis were used to compare the CT features among different World Health Organization (WHO) tumor pathological grades grades. Results: The following pathological diagnoses were obtained in the 50 pNENs patients: 24 patients had G1 neuroendocrine tumors (NETs), 5 patients had G2 NETs, and 21 had G3 neuroendocrine carcinomas (NECs). The majority of G2 and G3 tumors were poorly defined and lobular in shape and were larger than G1 tumors. Cystic necrosis, pancreatic duct dilatation, bile duct dilatation, peripancreatic tissue or vascular invasion, lymphadenopathy and distant metastasis were absent in most G1 tumors. Tumor size, TNM stage (III), poorly defined margins, and heterogeneous density on contrast-enhanced CT had the highest sensitivity of 95.2% for distinguishing between G3 tumors and G1/2 tumors, while irregular shape had the highest specificity of 89.7%, with a sensitivity of 85.7%. Conclusions: Several CT features were verified as predictors of the pathological tumor classification of pNENs with a high sensitivity and specificity.

Keywords: Pancreatic neuroendocrine neoplasms, computed tomography, pathological classification

Introduction

Pancreatic neuroendocrine neoplasms (pNENs), which originate from pluripotent stem cells, account for only 1-2% of cases of pancreatic cancer and are divided into functional and non-functional pancreatic neuroendocrine tumors based on clinical symptoms [1, 2]. Based on secretin, functioning pNENs can be classified into insulin-secreting tumors, gastrinomas, glucagon-secreting tumors, somatostatinomas, vasoactive intestinal peptide tumors, etc [3]. It is difficult to increase the understanding and improve the diagnostic accuracy of pNENs due

to the lack of unique clinical symptoms, especially in nonfunctional pNENs [4, 5]. Based on the histopathological determination of biological aggressiveness, the WHO classified pNENs into 3 grades as follows: grade 1 neuroendocrine tumors (G1 NETs), grade 2 NETs (G2 NETs), and grade 3 neuroendocrine carcinomas (G3 NECs) in 2010 [6]. According to the 2016 national Comprehensive Cancer Network guidelines, patients with different grade tumors should to receive specific treatments [7]. Surgical resection is recommended for resectable G1/G2 NETs; surgical resection or targeted molecular therapy can be used for metastat-

ic G1/G2 NETs; and platinum-based chemotherapy is a better treatment for metastatic G3 NECs.

For histopathological examinations of invasiveness and hysteresis, several diagnostic methods have been developed. Immunohistochemical analysis can be used as a diagnostic method; however, there are no specific markers available to distinguish G3 NECs from G1/2 NETs [8]. Medical imaging techniques are widely used to identify primary tumors, assess tumor scope, determine therapy, and provide a follow-up assessment after treatment; these techniques mainly include endoscopic ultrasonography [9], computed tomography (CT) [10], and magnetic resonance imaging (MRI) [11]. CT is the gold standard for localizing malignant pNENs and for identifying pancreatic atrophy and regional lymph node enlargement, with a sensitivity of approximately 90% [12].

The aim of this study was to analyze the CT features of pNENs and the relationship of these features to pathological classifications and to recognize useful imaging features for identifying G1, G2 and G3 tumors. The results indicated that CT features were essential clues for identifying different WHO grades of pNENs.

Materials and methods

Patient selection

This study was conducted with approval from the institutional review board of our hospital. All procedures involving human participants were performed in accordance with the ethical standards of the institutional research committee and with the 1964 Helsinki Declaration and its later amendments or comparable ethical standards. Our institutional review board approved the retrospective study, and 50 pNENs patients diagnosed by postoperative pathology in our hospital from September 2012 to July 2016 were included in the study. The inclusion criteria were as follows: 1) patients who underwent surgery and had histopathology performed following surgery; and 2) patients who underwent plain and contrast-enhanced CT without any treatment prior to surgery. This study included 27 men and 23 women with an average age of 48.52±14.96 years (range from 18 to 73 years).

The clinical symptoms of the patients were as follows. Fourteen of the 15 patients with functional pNENs had endocrine symptoms, such as glycopenia, recurrent dizziness, blurred vision, unconsciousness, intermittent palpitations, hypodynamia, and sweating. One patient with a glucagonoma had hyperglycemia for 17 years that was accompanied with weight loss, without obvious dry mouth or polydipsia. Twenty-nine of the 35 patients with nonfunctional pNENs had atypical symptoms, such as intermittent abdominal pain, abdominal distension, diarrhea, pyrexia, vomiting, lumbago and backache. Six patients had no obvious symptoms, and their diseases were discovered incidentally on routine physical examinations. All the tumors were then classified on histopathology as G1, G2, or G3 based on the WHO standards [6], and the disease was staged with the TNM staging system [13]. The demographic and clinical data are shown in **Table 1**.

CT image acquisition

CT examinations were performed using a 64-slice spiral CT system (SIEMENS SOMATOM Definition AS+, Siemens, Germany) or a 320-slice spiral CT system (TOSHIBA Aquilion ONE, Toshiba Medical System, Tokyo, Japan). All patients were asked to fast for eight hours before the CT scan. Patients consumed approximately 500-800 ml of drinking water to expand the stomach and duodenum 30 mins before the scan and an additional 250-300 ml of drinking water just before the scan. When the scan began, patients were in a supine position and held their breath.

The CT imaging parameters were as follows: tube voltage, 120 kV with automation current; section thickness, 5 mm; beam pitch, 1; SFOV (scanning field of view), 36 c; matrix, 512×512; and beam collimation, 128×0.6 mm (SIEMENS SOMATOM Definition AS+) or 100×0.5 mm (TOSHIBA Aquilion ONE). For contrast-enhanced CT, Ultravist 300 (Bayer Schering Pharma, Berlin, Germany) was administered intravenously at a rate of 2.5 ml/sec using a high-pressure injector at a dose of 1.5 ml/kg body weight. The arterial and portal venous phase scans were obtained at 30-35 second and 55-60 second delays, respectively.

Table 1. General information of patients with pNENs

| | Pathological classification | | | | F/χ^2 | P |
	G1	G2	G3	Total		
Sex					10.68	0.005*
Male	11 (40.74%)	0 (0%)	16 (59.26%)	27		
Female	13 (56.52%)	5 (21.74%)	5 (21.74%)	23		
Age	45.04±14.32	53.00±17.71	51.43.86±14.88	48.52±14.96	1.29	0.286
Hormonal syndrome					18.41	<0.001*
Functional	14 (93.33%)	1 (6.67%)	0	15		
Nonfunctional	10 (28.57%)	4 (11.43%)	21 (60%)	35		
Pancreatic location					6.57	0.583
Head	12 (40%)	5 (16.67%)	13 (43.33%)	30		
Neck	3 (75%)	0 (0%)	1 (25%)	4		
Body	5 (55.56%)	0 (0%)	4 (44.44%)	9		
Tail	4 (66.67%)	0 (0%)	2 (33.33%)	6		
TNM stage					40.58	<0.001*
I	15 (100%)	0 (0%)	0 (0%)	15		
II	5 (55.56%)	3 (33.33%)	1 (11.11%)	9		
III	4 (25%)	2 (12.5%)	10 (67.5%)	16		
IV	0 (0%)	0 (0%)	10 (100%)	10		

*$P<0.05$.

CT imaging analysis

The pathological diagnoses were made by 2 associate chief physicians who were aware of the presence of pNENs but were blinded to the grades. They reported the following observations [14]: tumor location, shape, tumor size, margins, growth pattern, cystic necrosis, calcification, pancreatic atrophy, pancreatic duct dilatation, bile duct dilatation, tissue or blood vessel involvement, lymphatic metastasis and distant metastasis. The pNENs patterns were divided into solid, solid and cystic, complex cystic and cystic, according to a previous report [14]. The CT attenuation values were determined as follows. Two-thirds of the solid tumor was included as a region of interest (ROI) and the CT values were measured according the following rules: 1) The contrast enhancement of the neoplasm-to-pancreas of pNENs was compared. The unenhanced phase, arterial phase, and portal venous phase CT attenuation values were recorded as NP, NA, NV in the center of the neoplasm and as PP, PA, PV in the peripheral pancreas, respectively. 2) The CT attenuation values of the tumors were subsequently measured in the largest parts of the lesions that showed relatively homogeneous attenuation, avoiding calcified regions in the tumors, cystic areas, and adjacent normal vasculature.

3) The values were measured in triplicate, and the average values were calculated. 4) The data were calculated according to previous reports [15], and the calculations are shown as follows:

A1 (absolute tumor enhancement in the arterial phase) = NA-NP; A2 (absolute pancreatic enhancement in the arterial phase) = PA-PP; A (ratio of the relative enhancement in the arterial phase) = A1/A2; V1 (absolute tumor enhancement in the portal venous phase) = NV-NA; V2 (absolute pancreatic enhancement in the portal venous phase) = PV-PA; V (ratio of the relative enhancement in the portal venous phase) = V1/V2; RA (relative enhancement in the arterial phase) = NA-PA; and RV (relative enhancement in the portal venous phase) = NV-PV.

Statistical analysis

To determine whether or not there was a significant difference in the demographic characteristics between G1, G2 and G3 tumors, ANOVA or the Kruskal-Wallis test was used for comparing continuous variables. The general information of the patients, CT features, and CT values for pathological classification of pNENs were analyzed using the χ^2 test or

Table 2. Relationship between CT features and pathological classification of pNENs

	Pathological classification				F/χ^2	P
	G1	G2	G3	Total		
Tumor size	2.33±1.41	5.70±2.13	5.46±1.95	3.98±2.33	21.20	<0.001*
Size					28.65	<0.001*
≤2 cm	15 (100%)	0 (0%)	0 (0%)	15		
2-4 cm	6 (50%)	2 (16.67%)	4 (33.33%)	12		
>4 cm	3 (13.04%)	3 (13.04%)	17 (73.91%)	23		
Tumor shape					28.63	<0.001*
Round	22 (75.86%)	4 (13.79%)	3 (10.34%)	29		
Lobular	2 (9.52%)	1 (4.76%)	18 (85.71%)	21		
Margins					30.36	<0.001*
Well-defined	19 (76%)	5 (20%)	1 (4%)	25		
Poorly defined	5 (20%)	0 (0%)	20 (80%)	25		
Growth pattern					11.34	0.003*
Internal growth	10 (90.91%)	1 (9.09%)	0 (0%)	11		
External invasion	14 (35.90%)	4 (10.26%)	21 (53.85%)	39		
Pattern					22.07	0.001*
Solid	17 (58.62%)	3 (10.34%)	9 (31.03%)	29		
Solid and cystic	13 (81.25%)	1 (6.25%)	2 (12.5%)	16		
Complex cystic	0 (0%)	1 (100%)	0 (0%)	1		
Cystic	4 (100%)	0 (0%)	0 (0%)	4		
Tumor attenuation on unenhanced CT					2.32	0.677
Low	9 (60%)	1 (6.67%)	5 (33.33%)	15		
Iso	13 (43.33%)	4 (13.33%)	13 (43.33%)	30		
High	2 (40%)	0 (0%)	3 (60%)	5		
Tumor attenuation in the arterial phase					1.08	0.898
Low	5 (50%)	1 (10%)	4 (40%)	10		
Iso	2 (40%)	0 (0%)	3 (60%)	5		
High	17 (48.57%)	4 (11.43%)	14 (40%)	35		
Tumor attenuation in the portal venous phase					2.27	0.686
Low	5 (55.56%)	0 (0%)	4 (44.44%)	9		
Iso	7 (58.33%)	1 (8.33%)	4 (33.33%)	12		
High	12 (41.38%)	4 (13.79%)	13 (44.83%)	29		
Tumor homogeneity on contrast-enhanced CT					17.12	<0.001*
Homogenous	15 (88.24%)	1 (5.88%)	1 (5.88%)	17		
Heterogeneous	9 (27.27%)	4 (12.12%)	20 (60.60%)	33		
Cystic necrosis					8.36	0.015*
Present	8 (29.63%)	3 (11.11%)	16 (59.26%)	27		
Absent	16 (69.57%)	2 (8.70%)	5 (21.74%)	23		
Calcification					1.53	0.465
Present	8 (57.14%)	2 (14.29%)	4 (28.57%)	14		
Absent	16 (44.44%)	3 (8.33%)	17 (47.22%)	36		
Pancreatic duct dilatation					7.93	0.019*
Present	6 (27.27%)	2 (9.10%)	14 (63.64%)	22		
Absent	18 (64.29%)	3 (10.71%)	7 (25%)	28		
Bile duct dilatation					9.33	0.009*
Present	0 (0%)	1 (12.5%)	7 (87.5%)	8		
Absent	24 (57.14%)	4 (9.52%)	14 (33.33%)	42		
Pancreatic atrophy					4.26	0.119
Present	2 (20%)	2 (20%)	6 (60%)	10		
Absent	22 (55%)	3 (7.5%)	15 (37.5%)	40		

Peripancreatic tissue or vascular invasion					16.14	<0.001*
Present	4 (18.18%)	2 (9.10%)	16 (72.73%)	22		
Absent	20 (71.43%)	3 (10.71%)	5 (17.86%)	28		
Lymphadenopathy					24.26	<0.001*
Present	0 (0%)	0 (0%)	13 (100%)	13		
Absent	24 (64.86%)	5 (13.51%)	8 (21.62%)	37		
Distant metastasis					17.26	<0.001*
Present	0 (0%)	0 (0%)	10 (100%)	10		
Absent	24 (60%)	5 (12.5%)	11 (27.5%)	40		

*$P<0.05$.

Table 3. Comparison of CT values and the pathological classification of pNENs

	Pathological classification				F	P
	G1	G2	G3	Total		
CT values of tumors (HU)						
Unenhanced phase	37.50±12.75	39.40±7.50	36.43±7.07	37.24±10.10	0.18	0.833
Arterial phase	96.29±41.15	105.00±43.78	82.90±22.41	91.54±34.89	1.25	0.296
Portal venous phase	77.75±27.15	117.80±33.34	82.52±16.88	83.76±26.26	5.80	0.006*
Absolute enhancement in the arterial phase	58.79±36.09	65.60±43.78	46.48±20.54	54.30±31.45	1.23	0.302
Absolute enhancement in the portal venous phase	-18.54±22.67	12.80±37.09	-0.38±22.69	-7.78±26.22	5.14	0.01*
Tumor-to-pancreas contrast (HU)						
Relative enhancement in the arterial phase	15.17±35.65	4.20±52.26	14.09±19.39	13.62±31.36	0.25	0.780
Relative enhancement in the portal venous phase	0.58±27.28	21.00±17.61	10.52±17.26	6.80±23.27	2.15	0.128
Ratio of relative enhancement in the arterial phase	1.52±0.73	1.33±0.83	1.66±0.71	1.56±0.72	0.48	0.624
Ratio of relative enhancement in the portal venous phase	2.89±9.07	-0.86±2.51	1.93±3.52	2.11±6.74	0.65	0.529

*$P<0.05$.

Table 4. Sensitivity and specificity of CT features for differentiating G3 from G1/2 pNENs

Features	Sensitivity (%)	Specificity (%)	Odds ratio	Confidence interval (%)
Tumor size (>2.95 cm)	95.20	69.00	1.85	1.30-2.64
TNM stage (III)	95.20	79.30	23.42	3.26-168.13
Irregular shape	85.70	89.70	52.00	9.41-287.34
Poorly defined margins	95.20	82.80	96.00	10.35-890.58
Heterogeneous density on contrast-enhanced CT	95.20	55.20	24.62	2.90-208.71
Cystic necrosis	76.20	62.10	5.24	1.49-18.34
Pancreatic duct dilatation	66.70	72.40	5.25	1.55-17.77
Peripancreatic tissue or vascular invasion	76.20	79.30	12.27	3.19-47.19

Fisher's exact test (**Tables 1**-**3**). Nonparametric tests (Kruskal-Wallis test) were used to evaluate the general information of the patients and the CT features (**Tables 1** and **2**). Parametric tests were used for CT values (**Table 3**).

The sensitivity and specificity of each CT feature was calculated using a receiver operating characteristic curve (ROC) analysis to distinguish between G3 and G1/2 tumors (**Table 4**). In addition, odds ratios with 95% confidence intervals were also calculated for each CT feature. All statistical analyses were performed with SPSS 22 (SPSS Inc., Chicago, IL, USA), and a *P* value less than 0.05 was considered a significant difference.

Results

Patient demographics

Fifty patients with pNENs were pathologically diagnosed as follows: 24 patients had G1 NETs, 5 patients had G2 NETs, and another 21 patients had G3 NECs. The demographic characteristics of the patients, i.e., age, sex, tumor
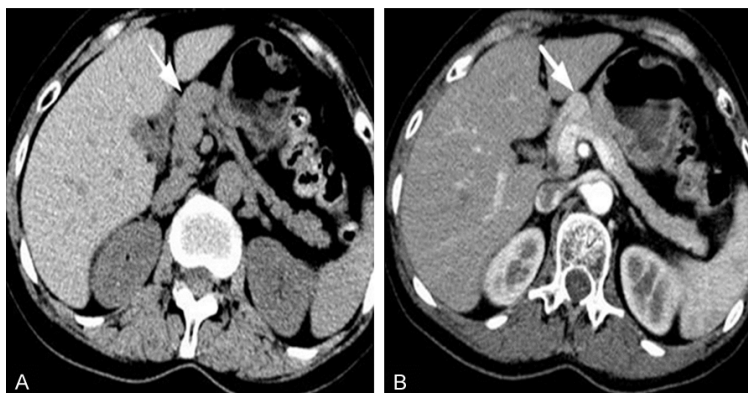
Figure 1. A 58-year-old woman with a benign nonfunctional pNEN that was classified as G1 and identified as a neuroendocrine tumor. A. Plain axial imaging showed an isodense quasi-circular lesion in the neck of the pancreas extending from the pancreas (arrow). B. Enhancement on arterial phase axial imaging showed uniform density of the foci with a clear border (arrow).
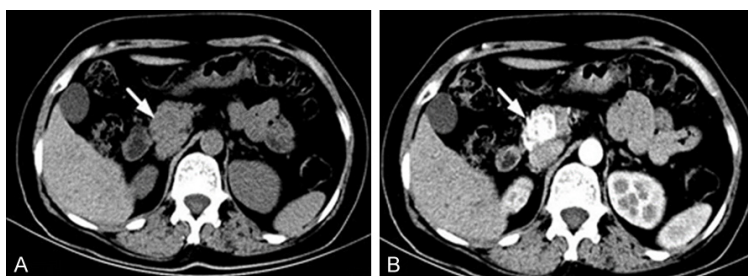

Figure 2. A 58-year-old woman with an islet cell adenoma that was classified as G2. A. Plain axial imaging showed an isodense quasi-circular lesion in the head of the pancreas head with a vague border (arrow). B. Enhancement on arterial phase axial imaging showed a focus with an obviously nonuniform density (arrow).
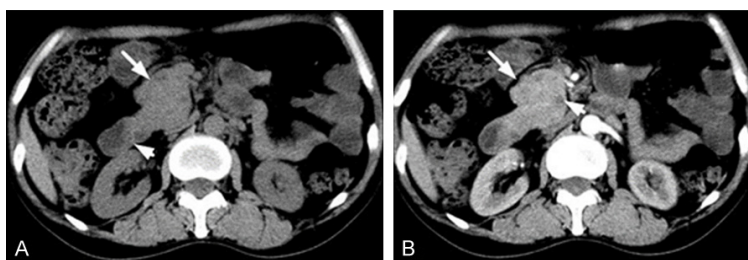
Figure 3. A 46-year-old woman with a malignant NEC with invasion of the duodenal papilla that was classified as G3. A. Plain axial imaging showed an isodense irregular shape at the head of the pancreas (arrow) growing outside of the pancreas with a vague border at the adjacent duodenal papilla (arrow head). B. Enhancement on arterial phase axial imaging showed a mildly nonuniform density at the foci (arrow) and multiple cystic lesions with uniform density (arrow head).

lence of different tumor grades was significantly different (*P*< 0.001) between functional and nonfunctional pNENs; grade 3 tumors were more likely to be nonfunctional pNENs. In addition, the same pattern existed among the TNM stages, with G2 and G3 tumors having higher TNM stages than G1 grade tumors (*P*<0.001).

Association of CT features and pathological classification of pNENs

Table 2 shows the association of the CT features among the different pathological grades of pNENs. Associations between tumor size, tumor shape, margins, growth pattern, pattern, tumor attenuation on unenhanced CT and in the arterial phase and the portal venous phase, tumor homogeneity on contrast-enhanced CT, cystic necrosis, calcification, pancreatic duct dilatation, bile duct dilatation, pancreatic atrophy, peripancreatic tissue or vascular invasion, lymphadenopathy, distant metastasis and the pathological classification of pNENs were statistically analyzed.

In the statistics analysis, growth pattern, pattern, cystic necrosis, pancreatic duct dilatation, and bile duct dilatation were significant predictors of the WHO classification. In addition, tumor size, margins, tumor shape, tumor homogeneity on contrast-enhanced CT, peripancreatic tissue or vascular invasion, lymphadenopathy, distant metastasis were stronger predictors compared with the other CT features.

grade, tumor location, the presence of hormonal syndrome and TNM stage, are shown in **Table 1**. There were no significant differences in age (*P* = 0.286) and tumor location (*P* = 0.583) among all the tumor grades. However, the preva-

Specifically, G2 and G3 tumors had a significantly larger tumor size than G1 tumors (*P*<0.001), while the majority of G1 tumors were round and well-defined and higher grade pNENs were poorly defined and lobular shaped.

Figure 4. A 25-year-old man with retroperitoneal lymphadenopathy that was classified as poorly differentiated neuroendocrine carcinoma (G3) associated with widespread metastatic foci. Enhancement on arterial phase axial imaging showed nonuniform density of the foci (arrow), in which cystic lesions were found, and the enlarged lymph nodes were significantly enhanced with nodosities (arrow head).
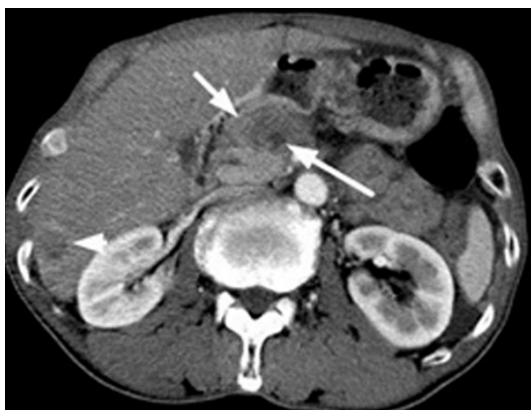

Figure 5. A 68-year-old man with liver metastasis that was classified as poorly differentiated neuroendocrine carcinoma (G3). Enhancement on portal venous phase axial imaging showed nonuniform density of the foci (short arrow) and cystic lesions with uniform density (long arrow). The metastatic liver foci showed boundary enlargement with a ring-like pattern (arrow head).

Regardless of the shape ($P<0.001$) and margins ($P<0.001$) of the tumor, pNENs with different grades showed significantly different patterns ($P = 0.003$). Moreover, the presence of cystic necrosis ($P = 0.015$), pancreatic duct dilatation ($P = 0.019$), bile duct dilatation ($P = 0.009$), peripancreatic tissue or vascular invasion ($P<0.001$), lymphadenopathy ($P<0.001$) and distant metastasis ($P<0.001$) were absent in the most patients with G1 tumors, whereas the presence of calcification ($P = 0.465$) and

pancreatic atrophy ($P = 0.119$) did not differ between tumors with different grades. No significant differences in tumor attenuation were observed between pNENs with different grades on unenhanced CT ($P = 0.677$) or in the arterial phase ($P = 0.599$).

Association of CT values and the pathological classification of pNENs

Quantitative comparisons of the CT values of different pathological tumor grades of pNENs are shown in **Table 3**. The mean contrast enhancement was significantly lower in the portal venous phase (P = 0.006) in G1 tumors than in G2/3 tumors; similarly, absolute enhancement in portal venous phase (P = 0.01), indicating vascularity, was lower in G1 tumors than in G2/3 tumors. No significant difference was observed in the tumor-to-pancreas contrast (P>0.05).

The CT characteristics in different grades are shown in **Figures 1-5**. **Figure 1** shows the CT images of a patient with a G1 tumor, **Figure 2** shows images from a patient with a G2 tumor, and **Figures 3-5** are from patients with G3 tumors. G1 tumors had uniform density and clear borders, while G3 tumors had nonuniform density and vague borders and associated invasion to peripheral organs (**Figure 3**), retroperitoneal lymph nodes (**Figure 4**), and distant metastasis (**Figure 5**). Metastatic foci were found in patients with G3 tumors, matching the finding of higher CT values in the portal venous phase in G3 tumors than in G1/2 tumors (**Table 3**).

Performance of CT features for diagnosing pNENs

Due to the different biological behaviors and medical treatments G1/2 and G3 pNENs, distinguishing G3 NECs from G1/2 tumors has great significance. The sensitivity and specificity of different CT features for differentiating G3 NECs from G1/2 pNENs were calculated and are listed in **Table 4**. A receiver operating characteristic (ROC) analysis was conducted to show the position of each cut-off value for the CT features listed in **Figure 6**. The highest odds ratio was achieved for poorly defined margins, irregular shape, density on enhancement, and TNM stage (III), and other features followed. Tumor size, TNM stage (III), poorly defined margins, and heterogeneous density on enhance-
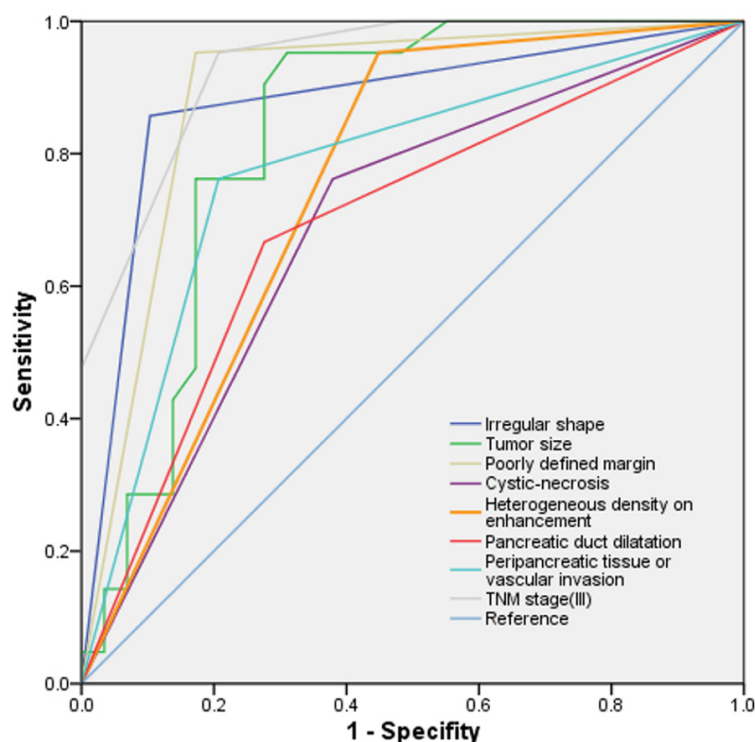
Figure 6. Receiver operating characteristic (ROC) analysis showing the position of each cut-off value for the CT features (irregular shape, tumor size, poorly defined margins, cystic necrosis, heterogeneous density on enhancement, pancreatic duct dilatation, peripancreatic tissue or vascular invasion, and TNM stage (III)).

Table 5. Sensitivity and specificity of computed tomography features for differentiating pathological tumor grades in recent studies

Features	Sensitivity (%)	Specificity (%)	Ref
Tumor size (>3 cm)	92.3	66.9	[14]
Poorly defined margins	15.4	99.4	[14]
Vascular invasion	46.2	94.8	[14]
Tumor size (>2 cm)	67	77	[15]
Tumor size (>2.9 cm)	83.3	92	[17]
Enhancement values in the pancreatic phase	91.7	84	[17]

logical classification. However, the diagnosis and classification of pNENs prove to be challenging, particularly when the lesion is smaller than 2 cm [4, 16]. Currently, medical imaging techniques play an important role in the diagnosis and classification of pNENs. Among these techniques, CT is particularly useful in identifying morphological changes, and previous studies have shown the usefulness of CT for identifying and localizing pancreatic tumors [14, 17-19].

The aim of this study was to determine whether the CT features of pNENs could facilitate differentiation between the WHO classifications. Plain and contrasted-enhanced CT features, such as tumor size, tumor shape, margins, growth pattern, pattern, tumor attenuation on unenhanced CT or in the arterial phase, tumor homogeneity on enhancement, cystic necrosis, calcification, pancreatic duct dilatation, bile duct dilatation, pancreatic atrophy, peripancreatic tissue or vascular invasion, lymphadenopathy, distant metastasis, were evaluated in relation to the pathological classification. Compared with previous reports [14, 15, 17], the largest number of CT features were measured and analyzed in this study. In this study, a higher grade was associated with a lobular shape, poorly defined margins, invasion outside the pancreas, malignancy, peripancreatic tissue or vascular invasion, lymphadenopathy and distant metastasis. Additionally, greater pancreatic duct dilatation and bile duct dilatation were present in higher grade tumors, especially in G3 tumors.

Furthermore, the diagnostic value of different CT features was also investigated in current study to distinguish G3 NECs from lower grade tumors. **Table 5** summarizes the sensitivity

ment showed the highest sensitivity of 95.2%, while irregular shape showed the highest specificity of 89.7%. Other features also showed satisfactory results in distinguishing G3 NECs from G1 or G2 pNENs (**Table 4**).

Discussion

The different biological behaviors of pNENs, ie, benign or malignant and resectable or unresectable, are highly associated with the patho-

and specificity of computed tomography features for distinguishing pathological tumor grades from recent studies. In this study, a tumor size with a cut-off value of 2.95 cm showed a sensitivity of 95.2% and a specificity of 69% for distinguishing G3 NECs from G1/2 NETs, which is the highest sensitivity and a similar specificity to those reported in previous CT studies [14, 15, 17] (**Table 5**). Moreover, irregular shape had the highest specificity of 89.7% for identifying G3 tumors in this study and was the best indicator for G3 tumors. Okabe H also suggested that shape was prognostic indicator for pNENs [18].

Plain axial CT imaging and enhancement in the arterial phase from three typical patients with different classifications of G1, G2 and G3 tumors are shown in **Figures 1-5**. Plain axial imaging only allowed the evaluation of shape, and G1 tumors were quasi-circular. When the enhancement in the arterial phase was used, the nonuniform density in grade 2 tumors showed some difference from grade 1 tumors. In patients with grade 3 tumors, nonuniform density, metastasis to peripheral organs and cystic degeneration were identified in the arterial phase. Higher grade tumors showed higher CT values and absolute enhancement in the portal venous phase. Previous reporters [20] have mentioned that contrast-enhanced CT is a feasible technique for assessing tumor vascularity [21], which is an important element for evaluating the biological aggressiveness of a tumor. The results in this study also indicated that contrast-enhanced CT could be used to estimate the biological aggressiveness of pNENs.

The presence of poorly defined margins, pancreatic duct dilatation and peripancreatic tissue or vascular invasion were common features in pancreatic ductal adenocarcinoma. Moreover, these features were also highly associated with G3 NECs in this study and the previous study [14]. A future study should evaluate the differences between G3 NECs and pancreatic ductal adenocarcinomas; endoscopic ultrasonography or MRI could be used as additional technologies [22, 23].

This retrospective study had several potential limitations. First, this study included a relatively small number of patients. Second, there were only 5 G2 pNENs according to the recent WHO classification. Third, this retrospective study lacked values from delayed phases on CT, which

limited the ability to compare the characteristics of the enhancement curves and differentiate iso/hypoattenuating pNENs from pancreatic ductal adenocarcinomas.

In conclusion, several plain and contrast-enhanced CT features (tumor size, tumor shape, vascular invasion, lymphadenopathy, distant metastasis, and absolute enhancement in the portal venous phase) can predict the pathological tumor classification of pNENs.

Disclosure of conflict of interest

None.

Address correspondence to: Kai Wang, Department of Neurosurgery, The Affiliated Hospital of Inner Mongolia Medical University, Hohhot 0100-50, China. Tel: +8618004718083; E-mail: 12881-515@qq.com; Ping Han, Department of Radiology, Union Hospital, Tongji Medical College, Huazhong University of Science and Technology, 1277 Jiefang Avenue, Wuhan 430022, China. Tel: +861370717-0023; E-mail: cjr.hanping@vip.163.com

References

[1] Siegel RL, Miller KD and Jemal A. Cancer statistics, 2017. CA Cancer J Clin 2017; 67: 7-30.

[2] Salaria SN and Shi C. Pancreatic neuroendocrine tumors. Surg Pathol Clin 2016; 9: 595-617.

[3] Crippa S, Partelli S, Boninsegna L and Falconi M. Implications of the new histological classification (WHO 2010) for pancreatic neuroendocrine neoplasms. Ann Oncol 2012; 23: 1928.

[4] Ito T, Hijioka S, Masui T, Kasajima A, Nakamoto Y, Kobayashi N, Komoto I, Hijioka M, Lee L, Igarashi H, Jensen RT and Imamura M. Advances in the diagnosis and treatment of pancreatic neuroendocrine neoplasms in Japan. J Gastroenterol 2017; 52: 9-18.

[5] Baur AD, Pavel M, Prasad V and Denecke T. Diagnostic imaging of pancreatic neuroendocrine neoplasms (pNEN): tumor detection, staging, prognosis, and response to treatment. Acta Radiol 2016; 57: 260-70.

[6] Lynch PM, Morris JS, Wen S, Advani SM, Ross W, Chang GJ, Rodriguez-Bigas M, Raju GS, Ricciardiello L, Iwama T, Rossi BM, Pellise M, Stoffel E, Wise PE, Bertario L, Saunders B, Burt R, Belluzzi A, Ahnen D, Matsubara N, Bulow S, Jespersen N, Clark SK, Erdman SH, Markowitz AJ, Bernstein I, De Haas N, Syngal S and Moeslein G. A proposed staging system and stage-specific interventions for familial adenomatous polyposis. Gastrointest Endosc 2016; 84: 115-125, e4.

[7]   Koh WJ, Greer BE, Abu-Rustum NR, Campos SM, Cho KR, Chon HS, Chu C, Cohn D, Crispens MA, Dizon DS, Dorigo O, Eifel PJ, Fisher CM, Frederick P, Gaffney DK, Han E, Higgins S, Huh WK, Lurain JR 3rd, Mariani A, Mutch D, Nagel C, Nekhlyudov L, Fader AN, Remmenga SW, Reynolds RK, Tillmanns T, Ueda S, Valea FA, Wyse E, Yashar CM, McMillian N and Scavone J. Vulvar cancer, version 1.2017, NCCN clinical practice guidelines in oncology. J Natl Compr Canc Netw 2017; 15: 92-120.

[8]   Yao JC, Pavel M, Lombard-Bohas C, Van Cutsem E, Voi M, Brandt U, He W, Chen D, Capdevila J, de Vries EG, Tomassetti P, Hobday T, Pommier R and Oberg K. Everolimus for the treatment of advanced pancreatic neuroendocrine tumors: overall survival and circulating biomarkers from the randomized, phase III RADIANT-3 study. J Clin Oncol 2016; 34: 3906-3913.

[9]   Palazzo M. Role of contrast harmonic endoscopic ultrasonography in other pancreatic solid lesions: neuroendocrine tumors, autoimmune pancreatitis and metastases. Endosc Ultrasound 2016; 5: 373-376.

[10]   Pruthi A, Pankaj P, Verma R, Jain A, Belho ES and Mahajan H. Ga-68 DOTANOC PET/CT imaging in detection of primary site in patients with metastatic neuroendocrine tumours of unknown origin and its impact on clinical decision making: experience from a tertiary care centre in India. J Gastrointest Oncol 2016; 7: 449-61.

[11]   Lotfalizadeh E, Ronot M, Wagner M, Cros J, Couvelard A, Vullierme MP, Allaham W, Hentic O, Ruzniewski P and Vilgrain V. Prediction of pancreatic neuroendocrine tumour grade with MR imaging features: added value of diffusion-weighted imaging. Eur Radiol 2017; 27: 1748-1759.

[12]   Dromain C, Deandreis D, Scoazec JY, Goere D, Ducreux M, Baudin E and Tselikas L. Imaging of neuroendocrine tumors of the pancreas. Diagn Interv Imaging 2016; 97: 1241-1257.

[13]   Cloyd JM and Poultsides GA. Non-functional neuroendocrine tumors of the pancreas: advances in diagnosis and management. World J Gastroenterol 2015; 21: 9512-25.

[14]   Kim DW, Kim HJ, Kim KW, Byun JH, Song KB, Kim JH and Hong SM. Neuroendocrine neoplasms of the pancreas at dynamic enhanced CT: comparison between grade 3 neuroendocrine carcinoma and grade 1/2 neuroendocrine tumour. Eur Radiol 2015; 25: 1375-83.

[15]   Takumi K, Fukukura Y, Higashi M, Ideue J, Umanodan T, Hakamada H, Kanetsuki I and Yoshiura T. Pancreatic neuroendocrine tumors: correlation between the contrast-enhanced computed tomography features and the pathological tumor grade. Eur J Radiol 2015; 84: 1436-1443.

[16]   Balachandran A, Tamm EP, Bhosale PR, Patnana M, Vikram R, Fleming JB, Katz MH and Charnsangavej C. Pancreatic neuroendocrine neoplasms: diagnosis and management. Abdom Imaging 2013; 38: 342-57.

[17]   Yamada S, Fujii T, Suzuki K, Inokawa Y, Kanda M, Nakayama G, Sugimoto H, Koike M, Nomoto S, Fujiwara M, Nakao A and Kodera Y. Preoperative identification of a prognostic factor for pancreatic neuroendocrine tumors using multiphase contrast-enhanced computed tomography. Pancreas 2016; 45: 198-203.

[18]   Okabe H, Hashimoto D, Chikamoto A, Yoshida M, Taki K, Arima K, Imai K, Tamura Y, Ikeda O, Ishiko T, Uchiyama H, Ikegami T, Harimoto N, Itoh S, Yamashita YI, Yoshizumi T, Beppu T, Yamashita Y, Baba H and Maehara Y. Shape and enhancement characteristics of pancreatic neuroendocrine tumor on preoperative contrast-enhanced computed tomography may be prognostic indicators. Ann Surg Oncol 2017; 24: 1399-1405.

[19]   Belousova E, Karmazanovsky G, Kriger A, Kalinin D, Mannelli L, Glotov A, Karelskaya N, Paklina O and Kaldarov A. Contrast-enhanced MDCT in patients with pancreatic neuroendocrine tumours: correlation with histological findings and diagnostic performance in differentiation between tumour grades. Clin Radiol 2017; 72: 150-158.

[20]   Bergers G and Benjamin LE. Tumorigenesis and the angiogenic switch. Nat Rev Cancer 2003; 3: 401-10.

[21]   Jia ZZ, Shi W, Shi JL, Shen DD, Gu HM and Zhou XJ. Comparison between perfusion computed tomography and dynamic contrast-enhanced magnetic resonance imaging in assessing glioblastoma microvasculature. Eur J Radiol 2017; 87: 120-124.

[22]   Manta R, Nardi E, Pagano N, Ricci C, Sica M, Castellani D, Bertani H, Piccoli M, Mullineris B, Tringali A, Marini F, Germani U, Villanacci V, Casadei R, Mutignani M, Conigliaro R, Bassotti G and Zullo A. Pre-operative diagnosis of pancreatic neuroendocrine tumors with endoscopic ultrasonography and computed tomography in a large series. J Gastrointestin Liver Dis 2016; 25: 317-21.

[23]   Manfredi R, Bonatti M, Mantovani W, Graziani R, Segala D, Capelli P, Butturini G and Mucelli RP. Non-hyperfunctioning neuroendocrine tumours of the pancreas: MR imaging appearance and correlation with their biological behaviour. Eur Radiol 2013; 23: 3029-39.